DOI: 10.1534/genetics.107.083295

Lethal Accumulation of Guanylic Nucleotides in *Saccharomyces cerevisiae HPT1*-Deregulated Mutants

Annick Breton,*,† Benoît Pinson,*,† Fanny Coulpier,‡ Marie-France Giraud,*,† Alain Dautant*,† and Bertrand Daignan-Fornier*,†,[1]

**Université Victor Segalen/Bordeaux 2, Institut de Biochimie et Génétique Cellulaires, 33077 Bordeaux, France,* †*CNRS, UMR 5095, 33077 Bordeaux, France and* ‡*IFR36, Plate-forme Transcriptome, École Normale Supérieure, 75230 Paris, France*

Manuscript received October 12, 2007
Accepted for publication November 30, 2007

ABSTRACT

Guanylic nucleotide biosynthesis is a conserved and highly regulated process. Drugs reducing GMP synthesis affect the immunological response and mutations enabling guanylic-derivative recycling lead to severe mental retardation. While the effects of decreased GMP synthesis have been well documented, the consequences of GMP overproduction in eukaryotes are poorly understood. In this work, we selected and characterized several mutations making yeast hypoxanthine–guanine phosphoribosyltransferase insensitive to feedback inhibition by GMP. In these mutants, accumulation of guanylic nucleotides can be triggered by addition of extracellular guanine. We show that such an accumulation is highly toxic for yeast cells and results in arrest of proliferation and massive cell death. This growth defect could be partially suppressed by overexpression of Rfx1p, a transcriptional repressor of the DNA damage response pathway. Importantly, neither guanylic nucleotide toxicity nor its suppression by Rfx1p was associated with an alteration of forward mutation frequency.

GUANYLIC nucleotides are required for synthesis of nucleic acids, metabolic reactions, and regulatory processes. In most organisms, GMP can be either synthesized from inosine 5′-monophosphate (IMP) or recycled from guanosine or guanine (Figure 1). In humans, impairment of either of these pathways leads to severe, although different, physiological consequences. Inhibitors of GMP synthesis from IMP affect lymphocyte proliferation and one of them, mycophenolate mofetil (CellCept, Roche), is commonly used as an immunosuppressive agent against transplantation rejection. Mutations blocking recycling of guanine and hypoxanthine by hypoxanthine–guanine phosphoribosyltransferase (HGPRT) result in hyperuricemia and in the most severe cases are associated with mental retardation and a compulsive self-mutilation behavior (Lesch–Nyhan syndrome) (Lesch and Nyhan 1964). Appropriate regulation of the guanylic nucleotide pools is thus a critical issue.

We use yeast as a model organism to study the metabolism of guanylic nucleotides (Figure 1) and their regulation. We have previously shown that transcription of the IMP dehydrogenase (IMPDH)-encoding genes (*IMD2*, *IMD3*, and *IMD4*) is strongly repressed by guanylic nucleotides (Escobar-Henriques and Daignan-Fornier 2001; Escobar-Henriques *et al.* 2003). We have also found that deletion of *HPT1*, the yeast HGPRT gene, leads to deregulation of the purine *de novo* pathway (Guetsova *et al.* 1997) and that mutations in the GMP kinase gene *GUK1* result in accumulation of GMP and mimic the *hpt1* deletion (Lecoq *et al.* 2000). These results combined with *in vitro* enzymatic studies allowed us to conclude that Hpt1p is feedback inhibited by GMP and that this regulation can indeed take place *in vivo*.

In this article, we describe the isolation and characterization of several mutations in *HPT1* that affect GMP feedback inhibition of yeast HGPRT. We propose a three-dimensional (3D) model for Hpt1p and show that several deregulated mutations are in the vicinity of the GMP-binding domain. Finally, we establish that deregulation of HGPRT leads to massive accumulation of guanylic nucleotides, which is highly deleterious for yeast cells.

MATERIALS AND METHODS

Strains and growth conditions: The *Saccharomyces cerevisiae* strains used in this study are listed in Table 1. Complete medium was YPD (1% yeast extract, 1% bactopeptone, 2% glucose). Minimal medium was SD (5% ammonium sulfate, 0.67% yeast nitrogen base Difco, 2% glucose). SD casa was SD supplemented with casaminoacids (0.2%). Other supplements were used at the following final concentration: guanine hydrochloride (0.3 mm), geneticine sulfate (G418) (0.2 g/liter), canavanine (60 mg/liter), 5-fluorocytosine (25 mg/liter), and doxycycline (10 mg/liter).

Plasmids: Centromeric plasmids [p2684 (*HPT1-1*), p2685 (*HPT1-3*), p2686 (*HPT1-7*), p2687(*HPT1-11*), and p2689 (*HPT1-16*)] containing the various *HPT1* alleles are derived from p386 (Guetsova *et al.* 1997), which carries the *HPT1*

[1]*Corresponding author:* Institut de Biochimie et Génétique Cellulaires, CNRS UMR 5095 1, rue Camille Saint-Saëns, 33077 Bordeaux Cedex, France. E-mail: b.daignan-fornier@ibgc.u-bordeaux2.fr

TABLE 1

Yeast strains used in this study

Strain	Genotype	Source
Y1026	*MAT*α *leu2-Δ0 his3-Δ1 lys2-Δ0 ura3-Δ0*	EUROSCARF
Y1656	*MAT*α *hpt1::kanMX4 leu2-Δ0 his3-Δ1 lys2-Δ0 ura3-Δ0*	EUROSCARF
Y1131	*MAT***a** *ade2::kanMX4 his3-Δ1 leu2-Δ0 met15-Δ0 ura3-Δ0*	EUROSCARF
Y2438	*MAT***a**	Fred Winston (FY4)
Y1715	*MAT***a** *ura3-52*	Fred Winston (FY3)
Y1708	*MAT***a** *trp1-Δ63*	Fred Winston (FY67)
Y1897	*MAT***a** *ura3-52 trp1-Δ63 leu2-Δ1*	Fred Winston (FY23)
m129	*MAT*α *guk1-1/ bra3-1 his3-Δ200 leu2-3,112 lys2-Δ201 ura3-52*	Guetsova *et al.* (1997)
m128	*MAT*α *ADE4-2/BRA11 his3-Δ200 leu2-3,112 lys2-Δ201 ura3-52*	Guetsova *et al.* (1997)
Y1711	*MAT*α *guk1-1 trp1-Δ63*	Lab collection
Y1712	*MAT***a** *guk1-1 ura3-52*	Lab collection
Y1705	*MAT***a** *ADE4-2 trp1-Δ63*	Lab collection
Y1726	*MAT*α *ADE4-2 trp1-Δ63*	Lab collection
Y1826	*MAT*α *guk1-1 ade2::kanMX4 leu2-3,112 ura3-52*	Lab collection
Y1868	*MAT***a** *hpt1::kanMX4 ura3-Δ0 trp1-Δ63*	Lab collection
Y1876	*MAT***a** *hpt1::kanMX4 ade2-101*	Lab collection
Y1961	*MAT***a** *HPT1-1, ura3-Δ0*	This work
Y1967	*MAT*α *HPT1-3 ura3-Δ0*	This work
Y324	*MAT***a** *HPT1-7 ura3-Δ0*	This work
Y1968	*MAT***a** *HPT1-11 ura3-Δ0*	This work
Y291	*MAT***a** *HPT1-16 ura3-Δ0*	This work
Y87	*MAT*α *hpt1::kanMX4, ura3-52::URA3-tet-HPT1-16 leu2 ura3 trp1-Δ63*	This work
Y3158	*MAT***a** *HPT1-16-tet-HPT1-16-URA3, ura3-Δ0*	This work

wild-type gene. Plasmids used for production of the Hpt1p protein in *Escherichia coli* were constructed as follows: the wild-type or mutant *HPT1* gene was amplified by PCR with oligonucleotides 961 GAGATTCCATATGTCGGCAAACGA TAAGCAA and 962 GACCTGCTCAGCTCGAGCTATCATTG CTTGTGTTCC. The PCR products were restricted by *Nde*I and *Bpu*1102I and ligated in the same restriction sites of pJC20-HisC (Lecoq *et al.* 2000), yielding the p3043 (*HPT1-1*), p3045 (*HPT1-3*), p3047 (*HPT1-7*), p3049 (*HPT1-11*), p3053 (*HPT1-16*), and p2890 (wild-type) plasmids. *Tet-HPT1* (p2149) and *tet-HPT1-16* (p2816) were constructed by amplification of the respective allele with oligonucleotides 551 CGCTGAT CAATGTCGGCAAACGATAAGCAA and 552 AAACTGCAG TCATTGCTTGTGTTCCTGCTC. The PCR fragments were restricted by *Bcl*I and *Pst*I and inserted in the *Bam*HI and *Pst*I sites of pCM189 (Gari *et al.* 1997). The integrative *tet-HPT1-16* plasmid (p2873) was constructed by replacement of the *CEN* region of p2816 by the *Nar*I–*Eco*RV fragment from YipLac211 (Gietz and Sugino 1988). The p3343 plasmid was isolated as a multicopy suppressor of guanine toxicity and p3359 (p3343Δ*Sma*I) and p3360 (p3343Δ*Sph*I) were obtained, from p3343, by restriction with the indicated enzyme and religation.

Mutagenesis: Mutations in the *HPT1* gene were generated in two independent PCR amplifications done with Taq DNA polymerase under mutagenic conditions (using two times lower concentration of dATP or dCTP than the other three dNTPs) with oligonucleotides 916 5′ GAAGCCGGATATAGT GAC 3′ and 917 5′ AAGTGCACCAGTAGACAC 3′. The PCR products were digested with *Eco*RV and cotransformed with p386 digested with *Sna*BI in the *guk1-1 ade2* double-mutant yeast strain (Y1826). This strain is unable to grow on hypoxanthine as a purine source due to feedback inhibition of Hpt1p by GMP (see results). Transformants were selected on SD casa plus adenine and replica plated twice on SD casa plus hypoxanthine. Twenty-two clones able to grow on hypoxanthine were selected among $>10^4$ transformants. Plasmids were extracted, amplified in *E. coli*, and sequenced. Several plasmids carried multiple mutations: the mutation K161R was recovered four times and the other single mutations once. The *HPT1* alleles were integrated into the yeast genome at the *HPT1* locus as follows. For each allelic form, an *Afl*III fragment carrying the *HPT1* gene was used to transform the Y1876 (*hpt1::kanMX4, ade2-101*). Transformants carrying gene replacement were selected as able to grow on hypoxanthine but unable to grow on G418. Finally, after mating with Y1656 (*hpt1::kanMX4, ADE2*), Ade^+ $G418^S$ meiotic segregants carrying the various alleles were obtained (Y1961, Y1967, Y324, Y1968, Y291). The *tet-HPT1-16* plasmid (p2873) was integrated either at the *ura3-52* locus (p2873 linearized with *Eco*RV) or at the *HPT1-16* (p2873 linearized with *Bam*HI).

Protein expression in *E. coli* and antibodies preparation: *E. coli* C41(DE3) (Miroux and Walker 1996) was transformed by p2890 containing the wild-type *HPT1* gene. Transformants were resuspended at OD_{600} 0.2 in 1 liter of LB medium containing 100 mg/liter of ampicillin and were grown at 30° for 1.5 hr. When the OD_{600} reached 0.8 unit, additional ampicillin (200 mg/liter final) and IPTG (1.5 mm) were added and cells were further grown for 3–6 hr at 30° to an OD_{600} of 4–5 units. Cells were then collected and resuspended in 50 ml Tris–HCl 20 mm, pH 8, NaCl 100 mm, lysozyme 100 μg/ml, PMSF 5 mm, DTT 2 mm. DNase (20 μg/ml) was added and incubated 15 min at room temperature, and then EDTA (2 mm) was added. The suspensions were cooled to 0° and homogenized in a sonicator. Cleared lysates were obtained after 1 hr centrifugation at 18,000 × *g*. The supernatant was brought to 0.65 m of ammonium sulfate, incubated for 1 hr at 4°, and centrifuged (20,000 × *g*, 30 min, 4°). The resulting supernatant was dialyzed against 2 × 1 liter of NaCl 20 mm, Tris–HCl 20 mm, pH 8.0, and the dialysate was loaded onto a Poros HQ/20 column. Proteins were eluted with a NaCl gradient and fractions containing a highly expressed 25-kDa protein were pooled and concentrated (Amicon unit, membrane

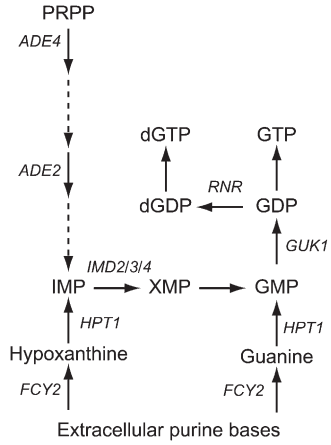

Figure 1.—Schematic of guanine nucleotide biosynthesis in yeast. Genes discussed in the text are italicized. IMP is inosine 5′-monophosphate, PRPP is 5-phosphoribosyl-1-pyrophosphate; and XMP is xanthosine 5′-monophosphate.

cutoff of 10,000 Da). The concentrate was brought to 1.33 M of ammonium sulfate and loaded on a POROS HP2/20 column equilibrated with ammonium sulfate 1.33 M, Tris–HCl 20 mM, pH 8.0. Proteins were eluted with a decreasing gradient of ammonium sulfate. After this second chromatographic step, a single protein band was visible after silver-stained SDS–PAGE. Mass spectrometry analyses confirmed this protein to be Hpt1p and revealed that the initial methionine was removed in bacteria. Rabbit polyclonal antibodies (Eurogentec) produced against the purified protein (four injections of 150 μg) reacted against a single protein of the expected size in Western blot experiments. No immunoreactive protein could be detected in a protein extract from the Δ*hpt1* strain.

For enzymatic assays, *E. coli* C41(DE3) transformed with the empty vector p1697 or with each of the *HPT1*-containing derivatives was grown in 100 ml. Extracts were prepared from the cleared lysates as described above. These extracts were then kept at −20° with protease inhibitors in 50% glycerol. SDS–PAGE separation and Coomassie staining of the extracts revealed that at least 50% of the total extract proteins resulted from a single band of the expected size (25 kDa) specifically induced by IPTG treatment and revealed by anti-Hpt1p antibodies. Staining intensity of this 25-kDa band was used to normalize Hpt1p levels in the enzymatic assay.

Enzymatic assay: HGPRT assays were performed as previously described (Lecoq *et al.* 2000) in a 50-μl mix containing 5-phosphoribosyl-1-pyrophosphate (PRPP) 100 μM, [8-^{3}H] hypoxanthine (1 mCi/ml, 20 Ci/mmol; Amersham, Piscataway, NJ) at a final concentration of 100 μM, yielding 51,300 dpm/nmol and 0, 100, 250, 500, or 1000 μM GMP. Reactions were started by adding 10 μl of the *E. coli* protein extracts diluted in such a way that no fewer than 1000 dpm were counted in any condition. For each extract, at least two series of experiments were done using two different dilutions. The reactions were stopped after 90 sec at 30°, and the product was precipitated and filtered on GF/C glass filters presoaked in 2 mM unlabeled hypoxanthine. Blanks were run in the same conditions, except that buffer replaced the extracts. Assays done with extracts prepared from *E. coli* containing the empty plasmid yielded no more activity than the blanks at the lowest dilution used.

Determination of intracellular guanine-derivative content: Cellular extracts were prepared by an ethanol extraction method adapted from the one described by Loret *et al.* (2007). Briefly, cells (25 ml/extraction) were grown to $OD_{600nm} = 1$ and harvested by rapid filtration on nitrocellulose filter (1 μm). The filter was immediately dropped into a glass tube containing 5 ml of ethanol/HEPES 10 mM, pH 7.2 (4/1), and the tube was then incubated at 80° for 3 min. The mixture was cooled down on ice for at least 3 min, and the ethanol/HEPES solution was then eliminated by evaporation using a rotavapor apparatus. The residue was resuspended in 500 μl of a 25-mM sodium pyrophosphate solution buffered at pH 5.7 with pyrophosphoric acid (PPi buffer). Insoluble particles were eliminated by centrifugation (12,000 × *g*, 10 min, 4°) and guanine-derivative content was determined by HPLC on the supernatant. Samples (20 μl) were injected on a C18 reverse-phase column (spherisorb ODS-2; 5 μm; 25 cm × 4.6 mm) equilibrated with PPi buffer, and the intracellular extracts were separated by isocratic elution in PPi buffer at constant flow (1.2 ml/min). Guanine derivatives, detected spectrophotometrically at 285 nm with a Gold 166 detection module (Beckman, Fullerton, CA), were identified by co-injection of purified guanine-derivatives standards (Sigma, St. Louis) and were quantified with the Gold quantification software (Beckman).

Molecular modeling: Secondary structures were predicted using the PSIPRED server (Bryson *et al.* 2005), and structure-based sequence alignment was drawn using ESPript (Gouet *et al.* 1999). Molecular modeling was carried out with Swiss model (Schwede *et al.* 2003), and ribbon diagram was drawn using MOLSCRIPT (Kraulis 1991).

DNA microarray analyses: Wild-type cells were transformed with a plasmid overexpressing the *HPT1-16* allele (p2816). Transformants were grown in SDcasaW medium in exponential phase for 24 hr at 30°. When the OD_{600} reached 0.7, the cell suspension was separated into two subcultures: one supplemented with 300 μM guanine (from a 30-mM solution in DMSO) and the other receiving only DMSO (control). The two subcultures were then grown at 30° and cells (50 ml/sample) were harvested by centrifugation after 15 and 30 min from each culture and immediately frozen at −80°. RNA was then extracted from cell pellets as described in http://www.transcriptome.ens.fr/sgdb/protocols/preparation_yeast.php# and were purified with an RNeasy purification kit (QIAGEN, Valencia, CA) according to the manufacturer's protocol. Labeling with Cy3 and Cy5 (2 μg of RNA/reverse transcription reaction) and cDNA probing on Agilent DNA microarray slides (GE 8 × 15K no. AMADID 015761) were done as described in http://www.transcriptome.ens.fr/sgdb/protocols/. The arrays were read with a Genepix 4000 scanner. Two hybridizations were performed for each comparison using the dye-swap procedure. Normalization was done with the lowess global method (Bengtsson *et al.* 2004).

RESULTS

Selection of feedback-resistant mutations in the *HPT1* gene: A genetic screen was designed to isolate mutations in *HPT1* that would lead to an HGPRT enzyme no longer feedback inhibited by GMP. The screen was based on the observation that a *guk1-1 ade2* double mutant is unable to use hypoxanthine as a purine source (Lecoq *et al.* 2000). The purine requirement is due to the *ade2* mutation that blocks the *de novo* pathway (Figure 1) while the inability to use hypoxanthine was shown to result from feedback inhibition of HGPRT by the GMP accumulated in strains carrying the *guk1-1* mutation (Lecoq *et al.* 2000). We reasoned that mutations in the *HPT1* gene that would

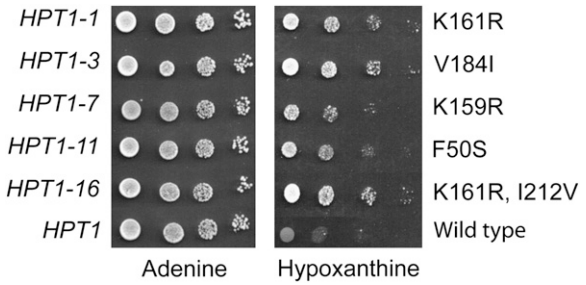

Figure 2.—Growth of an *ade2 guk1-1* double-mutant strain expressing various *HPT1* alleles. Yeast strain Y1826 (*ade2 guk1-1*) was transformed with p2684 (K161R), p2685 (V184I), p2686 (K159R), p2687 (F50S), p2689 (K161R, I212V), or p386 (wild type) plasmids. Aliquots of the various transformants were diluted in water to 10^7 cells/ml and serially diluted. Drops (5 μl) were deposited on SD casa + adenine or SD casa + hypoxanthine and cells were allowed to grow for 24 hr at 30°. Allele numbers and cognate amino acid substitutions are shown on the left and right, respectively.

make HGPRT feedback resistant should allow growth of *guk1-1 ade2* on hypoxanthine as a purine source. Since feedback-resistant mutants are generally dominant, the *HPT1* mutations were isolated in a strain carrying the wild-type allele at the *HPT1* locus. The *HPT1* gene, carried on a plasmid, was specifically mutated by error-prone PCR introduced into a *guk1-1 ade2* strain, and transformants able to grow on hypoxanthine were selected (see materials and methods).

For each transformant able to grow on hypoxanthine, the plasmids carrying the mutated *HPT1* gene were extracted and transformed back into the original *guk1-1 ade2* double-mutant strain and assayed again for growth on hypoxanthine. Sequencing of the *HPT1* gene in these plasmids revealed that they carry five different alleles of *HPT1* (Figure 2). All five mutations significantly improved growth of the *guk1-1 ade2* strain on hypoxanthine compared to the plasmid carrying the wild-type form of *HPT1*, although some alleles appeared stronger than others (Figure 2). Finally, the five mutations were reintroduced in the yeast genome at the *HPT1* locus (see materials and methods for details) and Western blot analyses confirmed that the mutations had no major effect on expression or stability of Hpt1p (data not shown).

***In vivo* effects of the *HPT1* feedback-resistant mutations:** Two *in vivo* assays were developed to ensure that these mutants are indeed true dominant feedback mutants. In a first assay, the phenotype considered was excretion of hypoxanthine in the medium by an *ADE4-2* mutant strain. The *ADE4-2* mutation makes the *de novo* pathway constitutively active and leads to overproduction of IMP, which is degraded to hypoxanthine by sequential action of Isn1p and Pnp1p (Lecoq *et al.* 2001; Rebora *et al.* 2001; Itoh *et al.* 2003). Overproduced hypoxanthine is massively excreted in the growth medium and excretion efficiency can be monitored by cross-feeding of a lawn of an *ade1* auxotrophic strain. Cross-feeding allows growth of the auxotrophic strain in the vicinity of the excreting mutant, the size of the growth halo being proportional to excretion efficiency. We reasoned that, under conditions where IMP is overproduced, hypoxanthine should be reused more efficiently by the HGPRT feedback-resistant mutants and less of it should be excreted in the medium. The *HPT1* mutants and the wild-type control strain were mated to a strain carrying the *ADE4-2* dominant mutation and the wild-type *HPT1* allele. The resulting diploids were assayed for purine excretion and, as expected, all the diploids carrying a *HPT1* mutation displayed a much smaller cross-feeding halo than the wild type (Figure 3A). Thus, the *HPT1* feedback mutants were able to reuse hypoxanthine more efficiently than the wild type, and, importantly, all the mutant alleles were dominant over the wild-type allelic form. Furthermore, this result strongly suggests that the *HPT1* feedback mutants, which were initially selected as resistant to feedback by GMP, are also resistant to feedback by IMP.

A second assay was aimed at evaluating the effect of the *HPT1* feedback-resistant mutations on accumulation of guanylic nucleotides, which are responsible for repression of IMPDH expression at the transcriptional level when cells are fed with guanine (Escobar-Henriques and Daignan-Fornier 2001). A plasmid carrying an *IMD2-lacZ* fusion was introduced in the wild-type and *HPT1* mutant strains and expression of the fusion was measured in the presence or absence of extracellular guanine. As expected, repression of *IMD2-lacZ* by guanine in the mutants was 2.5–3.7 times higher than in the wild-type strain (Figure 3B), indicating that guanylic nucleotides can substantially accumulate in the HGPRT-deregulated mutants. The strongest alleles were *HPT1-3* and *HPT1-16* (Figure 3B), as found previously for suppression of the *guk1-1 ade2* growth defect on hypoxanthine (Figure 2) and for hypoxanthine excretion (Figure 3A).

Mutations in HGPRT affect feedback inhibition by GMP *in vitro*: Wild-type and mutant alleles of *HPT1* overexpressed in *E. coli* were used to assay HGPRT activity *in vitro*. For all five mutated proteins, HGPRT activity was decreased by at least 50% when compared to wild-type levels (Figure 4A), indicating that the mutated residues interfere with the catalysis process even in the absence of feedback inhibition. Similar assays done in the presence of increasing amounts of GMP revealed that all the mutated enzymes were clearly less efficiently inhibited by GMP than the wild-type enzyme (Figure 4B). We conclude that, as expected, the mutant enzymes are more resistant to feedback inhibition by GMP than the wild type. Interestingly, the two strongest alleles *in vivo* (*HPT1-3* and *HPT1-16*; Figure 2; Figure 3, A and B) correspond to enzymes that did not loose too much activity compared to wild type (Figure 4A) and are strongly resistant to feedback inhibition (Figure 4B).

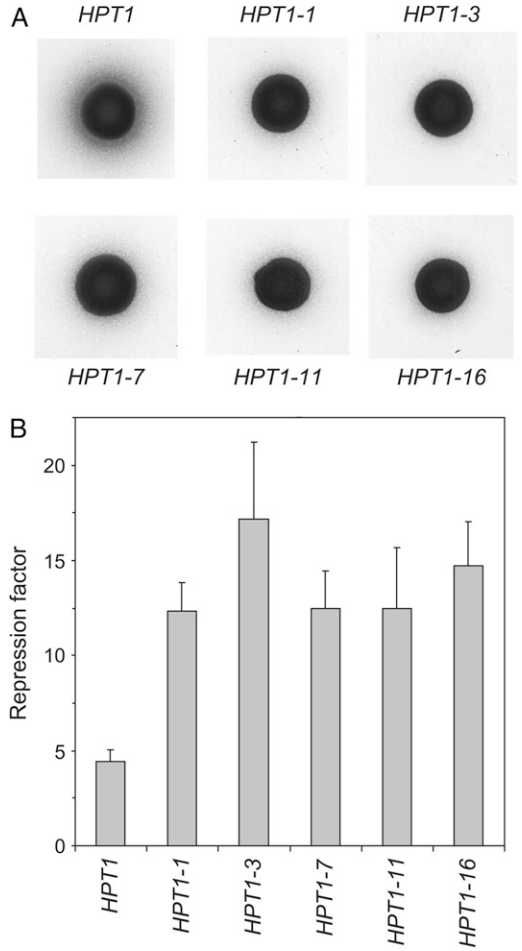

FIGURE 3.—*In vivo* effects of the *HPT1* feedback-resistant mutations. (A) Hypoxanthine excretion was monitored by the size of a halo of *ade1/ade1* on SD medium, surrounding a drop (5 μl of a suspension containing 10^7 cells/ml) of the diploids *ADE4-2*, *HPT1/ade4*, *HPT1-X*, as indicated. (B) Repression of *IMD2* by extracellular guanine in strains carrying the various *HPT1* alleles. The strains transformed with a plasmid bearing the *IMD2-lacZ* construct were grown in SD casa. Guanine (300 μM) was added to an aliquot of each culture for 6 hr. Initial cell density was 2×10^6 cells/ml. Expression from the *IMD2* promoter was evaluated by β-galactosidase assays. The ratio between the activity (in Miller units) in the absence and presence of guanine determines the repression factor for each strain. β-Galactosidase activities were in the same range in all cultures in the absence of guanine.

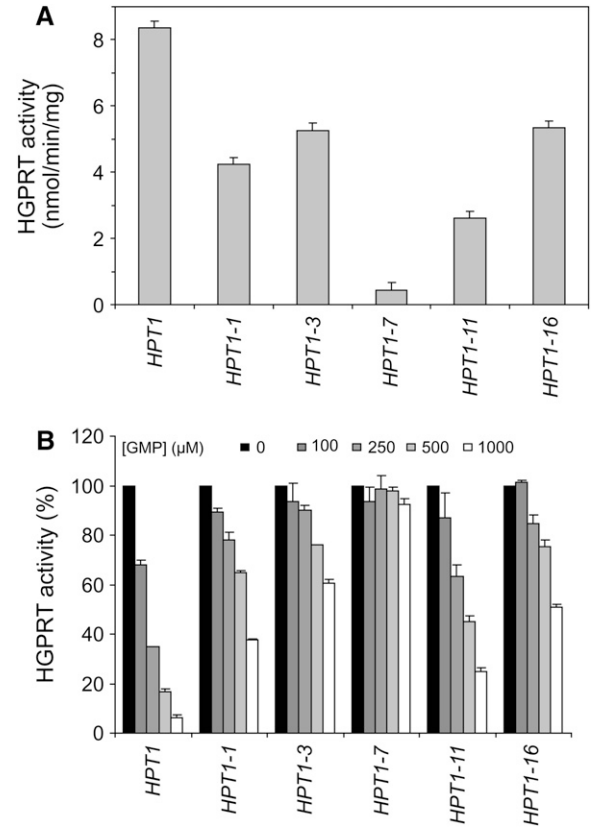

FIGURE 4.—Feedback inhibition of wild-type and mutant HGPRT. Enzymes were produced from *E. coli* and HGPRT activity was measured as described in MATERIALS AND METHODS with 100 μM of both hypoxanthine and PRPP. (A) HGPRT activity of the wild-type and mutant proteins. (B) Inhibition by GMP added at the indicated final concentrations. For each protein, HGPRT activities are displayed as a percentage of the activity measured in the absence of GMP.

Interestingly, *HPT1-1* and *HPT1-16* gene products share the K161R substitution, but in accordance with the *in vivo* effects, HGPRT from *HPT1-16* is more deregulated than that from *HPT1-1*. Therefore, the other substitution in *HPT1-16*, I212V, contributes to HGPRT deregulation. Together, our results show that the mutants retain a higher proportion of their HGPRT activity at high product concentration, compared to the wild type.

The Lys^{159}, Lys^{161}, and Val^{184} mutated residues are in the vicinity of the product-binding site in the 3D model of Hpt1p: To further understand how the feedback-resistant mutants affect HGPRT activity, we intended to obtain a 3D structure model for the yeast Hpt1p enzyme. Although HGPRT activity is strongly conserved in evolution, primary structures of yeast Hpt1p and mammalian or bacterial enzymes are not highly homologous. For example, Hpt1p shows only 12% identity (25% similarity) with the human enzyme (HPRT_HUMAN; PDB code: 1hmp; EADS *et al.* 1994) and 21% identity (37% similarity) with the presumed HGPRT from *Pyrococcus horikoshii OT3* reported by SUGAHARA and KUNISHIMA 2005 (O57827_PYRHO; PDB code: 1vdm). Due to this poor primary structure conservation, a secondary structure prediction was obtained for Hpt1p using PSIPRED and a structure-based alignment was then carried out with eight available HGPRT 3D structures (Figure 5A). This alignment revealed *P. horikoshii*-HGPRT as the closest relative to Hpt1p and this structure was therefore used to build the 3D model for Hpt1p (Figure 5B). It is clear, from this model, that Hpt1p adopts the "classical" PRTase folding with a core structure of a five-stranded parallel β-sheet surrounded by three α-helices. Importantly, two other PRTase-specific

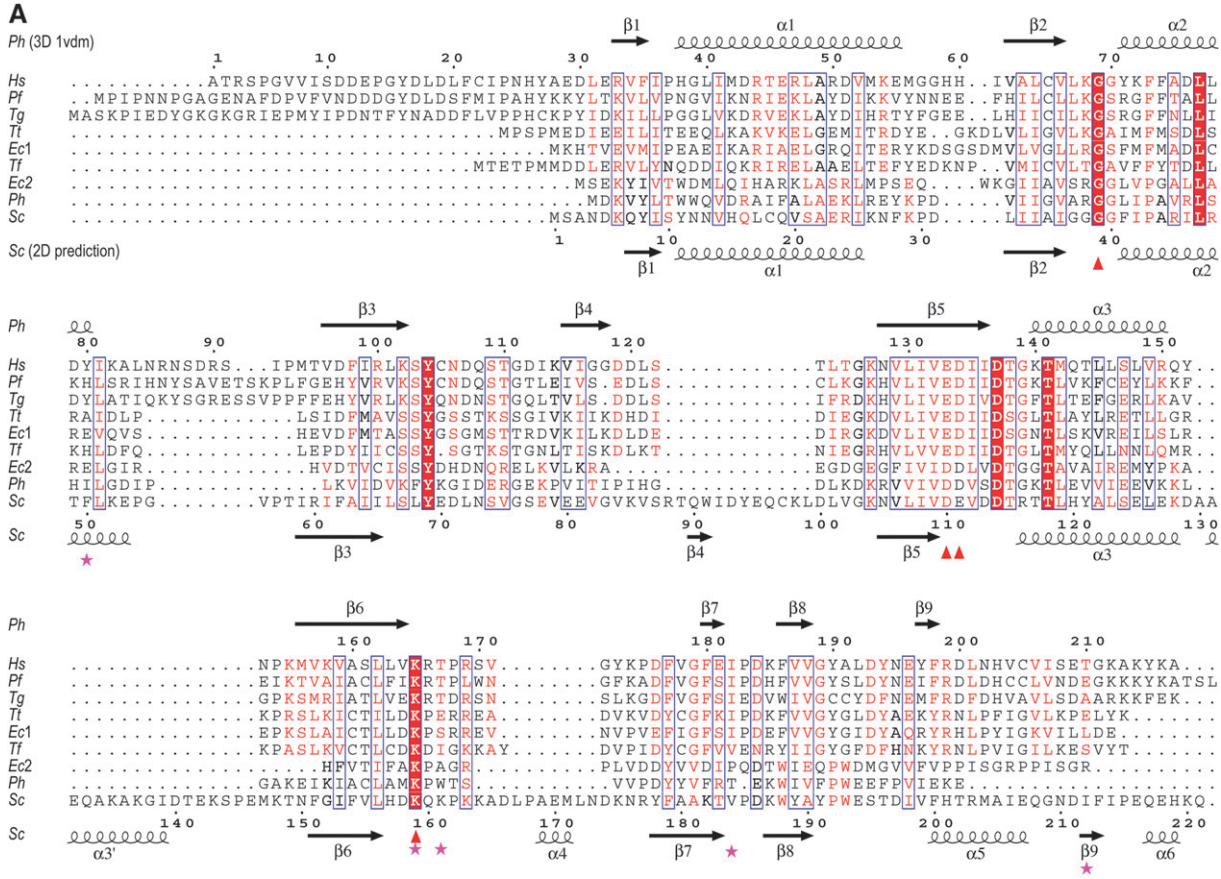
A
Ph (3D 1vdm)
Hs
Pf
Tg
Tf
Ec1
Tf
Ec2
Ph
Sc
Sc (2D prediction)
β1
α1
β2
α2
β3
β4
β5
α3
β6
β7
β8
β9
α3'
α4
α5
α6

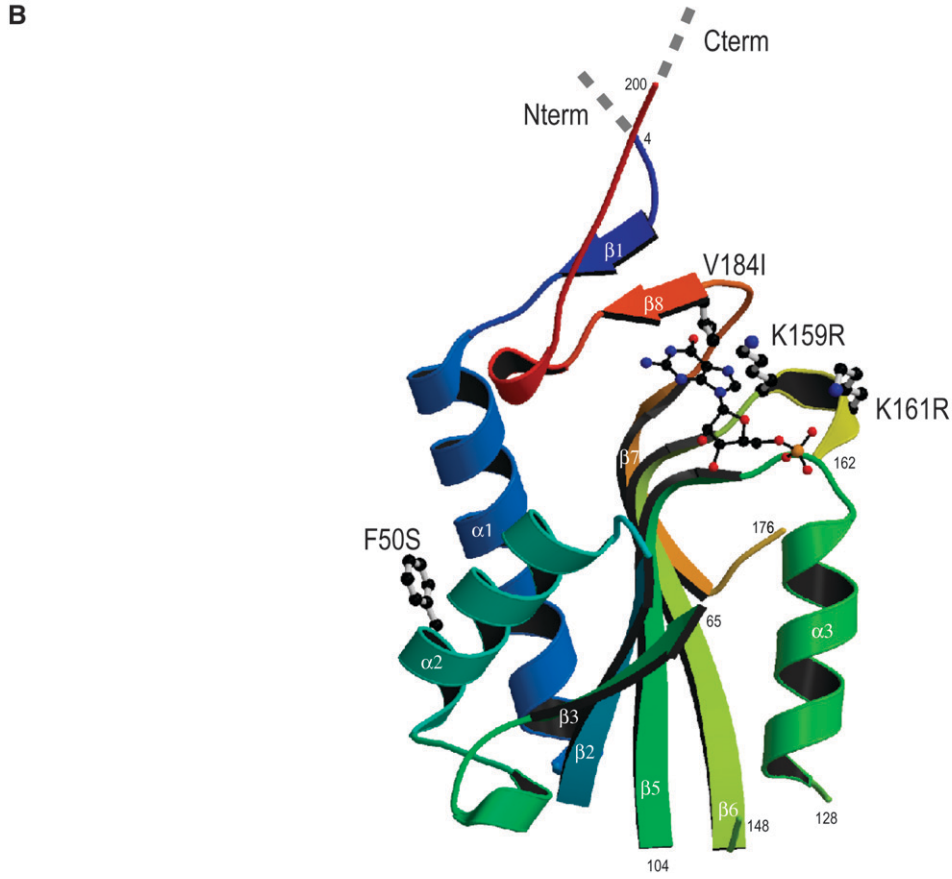
B
Cterm
Nterm
200
4
β1
V184I
β8
K159R
K161R
β7
162
176
F50S
α1
65
α3
α2
β3
β2
β5
β6
148
128
104

features were also found in the model. First, the Gly^{39} residue allowing a nonproline *cis*-peptide conformation required to accommodate a tight turn in the backbone is conserved. Second, the PRPP-binding-site motif (^{107}LIVDEVDDTR^{116}), named loop III, with the two conserved acidic residues, Asp^{110}-Glu^{111}, is present. Interestingly, a remarkable ^{188}WxxxPW^{191} motif, shared with the archael-, but not with mammalian- or prokaryote-HGPRT, is predicted as a strand that could form a parallel β-sheet with the β_1-strand of the N-terminal extremity. Finally, some unique features were found in the yeast enzyme. Three large insertions are notable in loop II (88–99), after the α_3-helix (130–146) and in the hood domain between residues 164 and 174. The C-terminal extension is predicted as an arm containing two helices and one strand (α_5, β_9, α_6). In addition to these particularities, our analysis based on secondary structure alignments argues for an overall conservation of the Hpt1p 3D structure, despite poor sequence homology.

The amino acid substitutions resulting in feedback resistance, when positioned on the model, were found in various regions of the protein. However, both K161R, the most frequent substitution, and V184I, corresponding to the other strong allele (*HPT1-3*), occur in the vicinity of the presumed GMP-binding site in the model (Figure 5B).

Overexpression of *HPT1-16* is lethal in the presence of extracellular guanine: We observed that the *HPT1-16* mutation leads to a slight growth defect specifically in the presence of guanine (Figure 6A). Overexpression of the wild-type *HPT1* gene, driven by the heterologous *tet* promoter, even more severely affected growth on guanine (Figure 6A). When transcriptional overexpression and feedback deregulation were combined, (*tet-HPT1-16* construct) growth in the presence of guanine was totally abolished, although a few colonies could grow (Figure 6A). Toxicity of guanine could be fully reversed by addition of doxycyclin, which turns down the *tet* promoter (Figure 6B).

The severe growth defect due to overexpression of *HPT1-16* in the presence of guanine was associated with a spectacular increase of cell death. After 24 hr in the presence of guanine, only ~5% of the *tet-HPT1-16* cells (Y3158) could form colonies, indicating that the rest of the cells were either dead or senescent. The percentage of dead cells in the culture (estimated by methylene blue staining of individual cells in two experiments; $n > 200$) was 3 ± 1 for the wild type, 44 ± 1 for the *tet-HPT1-16*, and 11 ± 2 for the *tet-HPT1-16* in the presence of doxycycline.

Analysis of intracellular guanylic nucleotide pools revealed that addition of extracellular guanine to a wild-type strain leads to a significant and rapid increase of GMP, GDP, and GTP intracellular concentrations (Figure 6C and supplemental Table 1 at http://www.genetics.org/supplemental/). The presence of the *tet-HPT1-16* construct did not significantly affect GMP concentration but resulted in a dramatic increase (more than fivefold) of both GDP and GTP concentration (Figure 6C). This effect was only partially reversed by doxycycline (Figure 6C). These results indicate that guanine toxicity associated with the *tet-HPT1-16* construct could be due to abnormal GDP and/or GTP concentration. Consistently, we found that the *tet-HPT1-16* construct was far less toxic in a GMP kinase mutant (*guk1-1*) that is affected in the synthesis of GDP from GMP (Figure 6D). We conclude that the toxicity of guanine, associated with the *tet-HPT1-16* construct, is a consequence of the drastic increase of GDP and/or GTP pools.

Finally, transcriptome analysis revealed that expression of >400 genes was affected by a factor two or more 30 min after guanine addition to a *tet-HPT1-16* strain. Among the most regulated genes (Figure 7), several purine metabolism genes were repressed, while genes involved in amino acid and energetic metabolism were induced. Upregulation of several genes involved in the stress response indicates that the toxic effect of guanine is perceived as a stress by yeast cells.

Overexpression of *RFX1* allows partial suppression of the *tet-HPT1-16* mutant growth defect: A search for genes that suppress the guanine toxicity when overexpressed was conducted from a strain carrying the *tet-HPT1-16* construct integrated at the *URA3* locus. We obtained several suppressor plasmids from two different genomic libraries. Further characterization of six plasmids revealed that five of them shared a common chromosomic region carrying only two complete open reading frames (*RFX1* and *YLR177w*). Further subcloning and retransformation revealed that *RFX1* was sufficient for suppression (Figure 8). Importantly, Western

Figure 5.—Position of the mutated residues in the HGPRT structure. (A) Multiple sequence alignment of Hpt1p with homologous proteins of known 3D structure. Numbering above sequences refers to the human sequence and numbering below the sequences refers to the *S. cerevisiae* sequence. Secondary structure elements based on the *P. horikoshii* PRTase crystal structure (PDB code 1vdm) and from 2D structure prediction for Hpt1p (PSIPRED) are drawn above and below the alignment, respectively. Residues forming the active site of human HGPRT and Hpt1p-mutated residues are highlighted with triangles and asterisks, respectively. *Hs, Homo sapiens* (HPRT_HUMAN); *Pf, Plasmodium falciparum* (HGXR_PLAFG); *Tg, Toxoplasma gondii* (HGXR_TOXGO); *Tt, Thermoanaerobacter tengcongensis* (Q8R7L0_THETN); *Ec*1, *E. coli* HPRT (HPRT_ECOLI); *Tf, Trichomonas fetus* (HGXR_TRIFO); *Ec*2, *E. coli* XGPRT (XGPT_ECOLI); *Ph, P. horikoshii OT3* (O57827_PYRHO); *Sc, S. cerevisiae* (HPRT_YEAST). (B) Ribbon representation of a 3D model of Hpt1p and localization of the mutated residues. The molecular modeling was performed from the HGPRT crystal structure of *P. horikoshii* (PDB code 1vdm chain A). GMP is represented on the model, as found in *Ec*-XGPRT structures complexed with this molecule (PDB code 1A97; Vos *et al.* 1997). Wild-type side chains of the mutated residues are drawn as ball and stick.

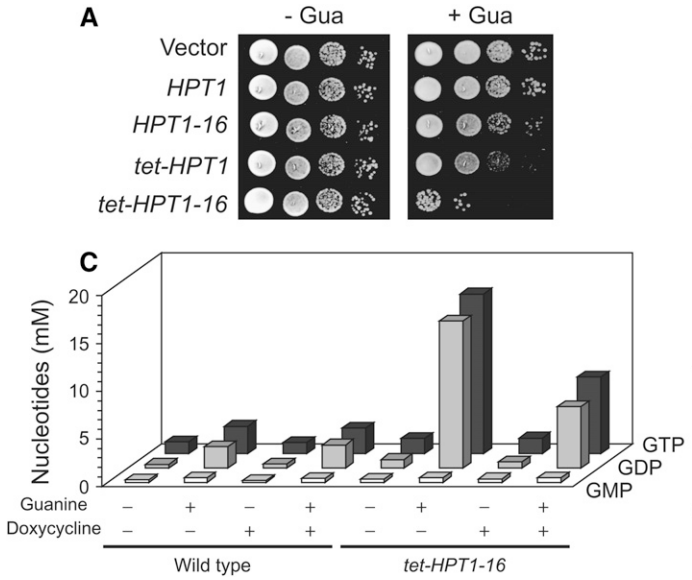

FIGURE 6.—Overexpression of *HPT1-16* is lethal in the presence of extracellular guanine. (A) Wild-type strain Y1026 was transformed with the indicated constructs and a serial dilution drop test was performed either on SD casa (−Gua) or on SD casa plus guanine (+Gua). (B) Y1026 was transformed with the *tet-HPT1-16* construct and a serial dilution drop test was performed on SD casa (−Gua) or SD casa plus guanine (+Gua), and doxycyclin was added when indicated (+Dox). (C) Y2438 (WT) or Y3158 (*tet-HPT1-16*) strains were grown in SD medium to 10^7 cells/ml. Intracellular GMP, GDP, and GTP content was determined by HPLC as described in MATERIALS AND METHODS (for numeric values see supplemental Table 1 at http://www.genetics.org/supplemental/). (D) Y1712 (*guk1-1*) strain was transformed with either the empty vector or the *tet-HPT1-16* construct, and a serial dilution drop test was performed on either SD casa (−Gua) or SD casa plus guanine (+Gua).

blot analysis showed that overexpression of *RFX1* did not affect *HPT1-16* expression driven by the *tet* promoter (data not shown).

RFX1 (*CRT1*) encodes a transcriptional repressor of the DNA damage response pathway (HUANG *et al.* 1998) homologous to the mammalian RFX family of DNA-binding proteins (REITH *et al.* 1990). Loss-of-function mutations in *RFX1* lead to constitutive expression of the ribonucleotide reductase (*RNR*)-encoding genes, while overexpression of Rfx1p results in non-inducible expression of *RNR3* (HUANG *et al.* 1998), indicating that Rfx1p levels are critical for *RNR* gene regulation. Ribonucleotide reductase, encoded by the *RNR* genes, is responsible for synthesis of dNDPs from NDPs precursors (Figure 1) and metabolizes GDP among other nucleotides. We thus wondered whether highly increased concentration of GDP in the *tet-HPT1-16* strain in the presence of guanine (Figure 6C) could result in increased dGTP concentration, which in turn could lead to unbalanced dNTPs pools and to massive mutagenesis.

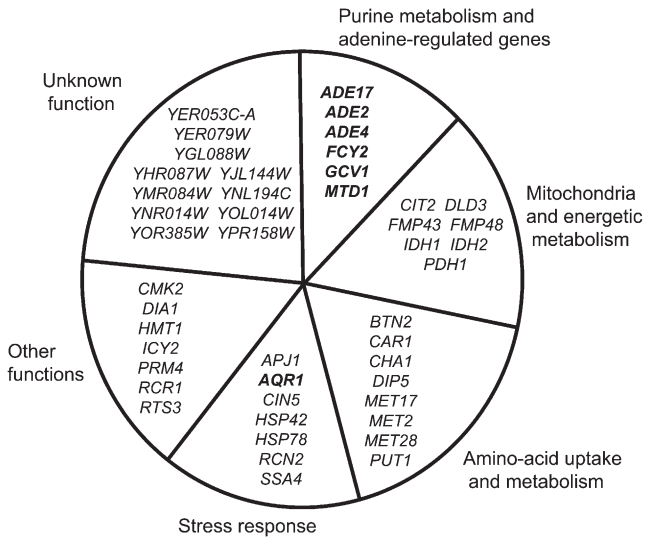

FIGURE 7.—Transcriptional response to guanine in cells overexpressing *HPT1-16*. Global transcriptional data were obtained on total RNA extracted from yeast cells grown in SDcasaW medium supplemented or not with guanine as described in MATERIALS AND METHODS. Genes listed in each category correspond to genes for which expression is induced (non-boldface type) or repressed (boldface type) more than threefold at both 15- and 30-min incubation times with guanine.

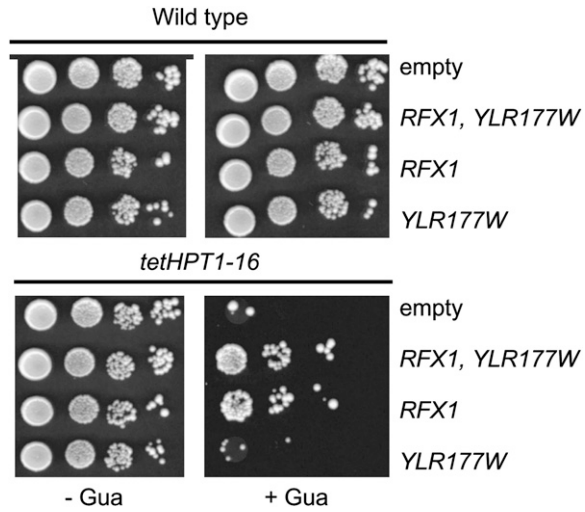

FIGURE 8.—Suppression of guanine toxicity by overexpression of *RFX1*. The wild-type (Y1708) and *tet-HPT1-16* (Y87) strains were transformed with the following plasmids: p2720 (empty), p3343 (*RFX1, YLR177W*), p3359 (*RFX1*), and p3360 (*YLR177W*) and then used for drop tests on either SD casa (−Gua) or SD casa + guanine (+Gua) media.

Mutant apparition frequency was monitored using canavanin or 5-fluorocytosine resistance assays in the wild-type and *tet-HPT1-16* strains, containing or not containing the *RFX1* overexpression plasmid and grown in the presence or absence of guanine. No significant mutagenic effect could be detected in any of these conditions (data not shown). Therefore, it is doubtful that suppression of guanine sensitivity is the result of increased mutagenesis.

DISCUSSION

In this work, we have isolated several mutations affecting feedback control of HGPRT by the reaction products. On the basis of our 3D model, we propose that the various mutations affect feedback regulation through distinct means.

A first group of three substitutions—K159R, K161R, and V184I—lead to increased steric hindrance in the GMP-binding crevice. Lys^{159}, which is mutated in *HPT1-7*, is equivalent to Lys^{165} in human HGPRT and is a highly conserved residue (Figure 5A). This residue interacts with the 6-oxo group of the guanine ring conferring 6-oxopurine base specificity (Craig and Eakin 2000). Consistent with the strong conservation of this residue, the HGPRT activity in the *HPT1-7* mutant is severely impaired. Poor interaction of this mutant protein with the reaction product could account for reduced feedback inhibition. The most frequently isolated mutation in our screen was K161R. Lys^{161} is not a conserved residue but, on the basis of our model, it could interact with the phosphate group of IMP or GMP. The longer lateral chain of arginine could possibly affect this interaction with the monophosphate moiety and thereby specifically affect product release. Another interesting case is Val^{184}, which belongs to a turn between the strands β_7 and β_8 close to the GMP-binding crevice. The bulky lateral chain of isoleucine in the mutant could disrupt the necessary movement of the aromatic side chains that interact with the purine base as deduced from the structure comparison of free and IMP- or GMP-complexed xanthine–guanine phosphoribosyltransferase (XGPRT) enzymes (Vos *et al.* 1997).

The reduced feedback inhibition due to mutations F50S and I212V (which enhances the effect of K161R in the *HPT1-16* mutant) could be due to altered oligomeric interactions. The Phe^{50} residue, which is mutated in *HPT1-11*, protrudes on the α_2-helix and Ile^{212}, mutated together with Lys^{161} in *HPT1-16*, belongs to the variable C-terminal arm that could not be positioned in our model. Equivalent regions in the *P. horikoshii* structure are involved in oligomerization. The oligomeric state of Hpt1p has not yet been established but HGPRTs are known to be usually functional as dimers or tetramers (Craig and Eakin 2000) and, in a specific case (*P. horikoshii* structure, PDB code: 1vdm), could be active as a hexamer.

Guanine nucleotide synthesis is tightly controlled at both the enzymatic and transcriptional levels. Cracking this double regulatory lock by overexpression of the feedback-resistant mutants of *HPT1* resulted in rapid growth arrest and cell death. These dramatic consequences for yeast cells were dependent on the presence of extracellular guanine and were associated with massive accumulation of both GDP and GTP in the cell. Accumulation of GDP and GTP, but not GMP, in the mutant clearly designates Hpt1p as the major regulatory step in the pathway, while downstream GMP- and NDP-kinase activities (Figure 1) are apparently not limiting. Partial suppression of the *tet-HPT1-16* toxicity by the *guk1-1* mutation, which limits GDP synthesis from GMP, points out guanylic nucleotide overdose as the cause of cell death. Importantly, total reversion of the guanine toxicity in the presence of doxycycline is associated with a limited decrease of GDP and GTP pools, indicating that yeast cells can tolerate a significant increase of guanylic nucleotide pools. Our finding that *RFX1* overexpression allows partial suppression of guanine effects might indicate that part of the toxicity takes place through DNA-damage-induced genes, which are downregulated by *RFX1* overexpression (Huang *et al.* 1998). Consistently, our microarray analysis revealed that *RNR3*, *HUG1*, and *PHR1*, three DNA-damage-induced genes, were induced two- to threefold in the *tet-HPT1-16* strain in the presence of guanine. Importantly, we found that the guanine toxicity and its suppression by *RFX1* overexpression were not associated with increased mutation frequency. This result suggests either that massive accumulation of GDP is not followed by dGTP overproduction or that such an overproduction does not affect mutation frequency.

Interestingly, excess of guanine nucleotides has been shown to affect *E. coli* growth (Petersen 1999). However, in this case, toxicity of guanosine in a guanosine kinase feedback mutant was dependent on conversion of GMP into IMP by GMP reductase and on guanosine 3′–5′-bispyrophosphate (ppGpp) accumulation (Petersen 1999). In *S. cerevisiae*, no GMP reductase homolog has been found and consistently guanine derivatives cannot be utilized for adenylic nucleotide synthesis. Furthermore, no role for ppGpp has ever been documented in yeast and it is thus likely that guanine nucleotide toxicity in *E. coli* and *S. cerevisiae* is due to different causes. Since guanine toxicity is largely reversed by a mutation in the GMP kinase gene, we believe that accumulation of some end product (GDP, GTP, or a derivative) is responsible for growth impairment. Since the balance between GXP and dGXP pools is largely influenced by RNR activity, which itself is regulated by Rfx1p, our results suggest that changes in dGXP pools could be important in the toxicity process, but that this should take place in a mutagenic-independent way.

It has been known for a long time that loss-of-function mutations in HGPRT lead to severe mental retardation, thus pointing to a crucial role for guanine recycling.

Likewise, mycophenolate derivatives that specifically block synthesis of GMP from IMP have antiproliferative and immunosuppressive effects (Shipkova *et al.* 2005). The consequences of reduced GMP synthesis or recycling have also been studied in yeast using mycophenolic acid (Escobar-Henriques *et al.* 2001) or HGPRT mutants (Guetsova *et al.* 1997). While all these studies reveal complex and critical roles for guanylic nucleotides, the consequences of GMP overproduction in eukaryotes had not been investigated before. The results presented here clearly show that overproduction of GMP derivatives leads to severe growth defect and massive cell death, thus establishing that overdose can be as detrimental as starvation. Our results on HGPRT show that, in this case, the purpose of negative feedback regulation is not restricted to adjustment of product abundance to cellular needs; indeed, proper regulation is critical for survival under conditions where the substrate is abundant.

The authors thank F. Lacroute for plasmid libraries, M. Bonneu for mass-spectrometry analysis, Laurent Jourdren for assistance with microarrays, and S. Saupe and L. Maillet for critical reading of the manuscript. This work was supported by grant no. 4749 from Association pour la Recherche sur le Cancer to B.D.-F.

LITERATURE CITED

Bengtsson, H., G. Jonsson and J. Vallon-Christersson, 2004 Calibration and assessment of channel-specific biases in microarray data with extended dynamical range. BMC Bioinformatics **5:** 177.

Bryson, K., L. J. McGuffin, R. L. Marsden, J. J. Ward, J. S. Sodhi *et al.*, 2005 Protein structure prediction servers at University College London. Nucleic Acids Res. **33:** W36–W38.

Craig, S. P., III, and A. E. Eakin, 2000 Purine phosphoribosyltransferases. J. Biol. Chem. **275:** 20231–20234.

Eads, J. C., G. Scapin, Y. Xu, C. Grubmeyer and J. C. Sacchettini, 1994 The crystal structure of human hypoxanthine-guanine phosphoribosyltransferase with bound GMP. Cell **78:** 325–334.

Escobar-Henriques, M., and B. Daignan-Fornier, 2001 Transcriptional regulation of the yeast gmp synthesis pathway by its end products. J. Biol. Chem. **276:** 1523–1530.

Escobar-Henriques, M., A. Balguerie, C. Monribot, H. Boucherie and B. Daignan-Fornier, 2001 Proteome analysis and morphological studies reveal multiple effects of the immunosuppressive drug mycophenolic acid specifically resulting from guanylic nucleotide depletion. J. Biol. Chem. **276:** 46237–46242.

Escobar-Henriques, M., B. Daignan-Fornier and M. A. Collart, 2003 The critical cis-acting element required for IMD2 feedback regulation by GDP is a TATA box located 202 nucleotides upstream of the transcription start site. Mol. Cell. Biol. **23:** 6267–6278.

Gari, E., L. Piedrafita, M. Aldea and E. Herrero, 1997 A set of vectors with a tetracycline-regulatable promoter system for modulated gene expression in Saccharomyces cerevisiae. Yeast **13:** 837–848.

Gietz, R. D., and A. Sugino, 1988 New yeast-*Escherichia coli* shuttle vectors constructed with *in vitro* mutagenized yeast genes lacking six-base pair restriction sites. Gene **74:** 527–534.

Gouet, P., E. Courcelle, D. I. Stuart and F. Metoz, 1999 ESPript: analysis of multiple sequence alignments in PostScript. Bioinformatics **15:** 305–308.

Guetsova, M. L., K. Lecoq and B. Daignan-Fornier, 1997 The isolation and characterization of *Saccharomyces cerevisiae* mutants that constitutively express purine biosynthetic genes. Genetics **147:** 383–397.

Huang, M., Z. Zhou and S. J. Elledge, 1998 The DNA replication and damage checkpoint pathways induce transcription by inhibition of the Crt1 repressor. Cell **94:** 595–605.

Itoh, R., C. Saint-Marc, S. Chaignepain, R. Katahira, J. M. Schmitter *et al.*, 2003 The yeast ISN1 (YOR155c) gene encodes a new type of IMP-specific 5′-nucleotidase. BMC Biochem. **4:** 4.

Kraulis, P. J., 1991 MOLSCRIPT: a program to produce both detailed and schematic plots of protein structures. J. Appl. Crystallogr. **24:** 946–950.

Lecoq, K., M. Konrad and B. Daignan-Fornier, 2000 Yeast GMP kinase mutants constitutively express AMP biosynthesis genes by phenocopying a hypoxanthine-guanine phosphoribosyltransferase defect. Genetics **156:** 953–961.

Lecoq, K., I. Belloc, C. Desgranges, M. Konrad and B. Daignan-Fornier, 2001 YLR209c encodes Saccharomyces cerevisiae purine nucleoside phosphorylase. J. Bacteriol. **183:** 4910–4913.

Lesch, M., and W. L. Nyhan, 1964 A familial disorder of uric acid metabolism and central nervous system function. Am. J. Med. **36:** 561–570.

Loret, M. O., L. Pedersen and J. Francois, 2007 Revised procedures for yeast metabolites extraction: application to a glucose pulse to carbon-limited yeast cultures, which reveals a transient activation of the purine salvage pathway. Yeast **24:** 47–60.

Miroux, B., and J. E. Walker, 1996 Over-production of proteins in Escherichia coli: mutant hosts that allow synthesis of some membrane proteins and globular proteins at high levels. J. Mol. Biol. **260:** 289–298.

Petersen, C., 1999 Inhibition of cellular growth by increased guanine nucleotide pools. Characterization of an Escherichia coli mutant with a guanosine kinase that is insensitive to feedback inhibition by GTP. J. Biol. Chem. **274:** 5348–5356.

Rebora, K., C. Desmoucelles, F. Borne, B. Pinson and B. Daignan-Fornier, 2001 Yeast AMP pathway genes respond to adenine through regulated synthesis of a metabolic intermediate. Mol. Cell. Biol. **21:** 7901–7912.

Reith, W., C. Herrero-Sanchez, M. Kobr, P. Silacci, C. Berte *et al.*, 1990 MHC class II regulatory factor RFX has a novel DNA-binding domain and a functionally independent dimerization domain. Genes Dev. **4:** 1528–1540.

Schwede, T., J. Kopp, N. Guex and M. C. Peitsch, 2003 SWISS-MODEL: an automated protein homology-modeling server. Nucleic Acids Res. **31:** 3381–3385.

Shipkova, M., V. W. Armstrong, M. Oellerich and E. Wieland, 2005 Mycophenolate mofetil in organ transplantation: focus on metabolism, safety and tolerability. Expert Opin. Drug Metab. Toxicol. **1:** 505–526.

Sugahara, M., and N. Kunishima, 2005 1vdm structure release at Protein Data Base. http://www.rcsb.org/.

Vos, S., J. de Jersey and J. L. Martin, 1997 Crystal structure of Escherichia coli xanthine phosphoribosyltransferase. Biochemistry **36:** 4125–4134.

Communicating editor: M. Johnston